MOLECULAR ONCOLOGY 6 (2012) 418–427

available at www.sciencedirect.com

SciVerse ScienceDirect

www.elsevier.com/locate/molonc

Effect of antiangiogenic therapy on tumor growth, vasculature and kinase activity in basal- and luminal-like breast cancer xenografts

Evita M. Lindholm[a,*], *Alexandr Kristian*[a], *Hawa Nalwoga*[b], *Kristi Krüger*[b], *Ståle Nygård*[c], *Lars A. Akslen*[b], *Gunhild M. Mælandsmo*[a,d], *Olav Engebraaten*[a,e]

[a]*Department of Tumor Biology, Institute for Cancer Research, Oslo University Hospital, The Norwegian Radium Hospital, Pb 4953 Nydalen, 0424 Oslo, Norway*

[b]*The Gade Institute, Section for Pathology, University of Bergen, 5020 Bergen, Norway*

[c]*Bioinformatics Core Facility, Institute for Medical Informatics, Pb 4953 Nydalen, 0424 Oslo, Norway*

[d]*Department of Pharmacy, Faculty of Health Sciences, University of Tromsø, 9037 Tromsø, Norway*

[e]*Department of Oncology, Oslo University Hospital, Ullevål and Institute of Clinical Medicine, University of Oslo, 0424 Oslo, Norway*

ARTICLE INFO

Article history:
Received 25 January 2012
Received in revised form
23 February 2012
Accepted 22 March 2012
Available online 31 March 2012

Keywords:
Angiogenesis
Bevacizumab
Breast cancer
Xenografts
Tumor vasculature
Kinase activity

ABSTRACT

Several clinical trials have investigated the efficacy of bevacizumab in breast cancer, and even if growth inhibiting effects have been registered when antiangiogenic treatment is given in combination with chemotherapy no gain in overall survival has been observed. One reason for the lack of overall survival benefit might be that appropriate criteria for selection of patients likely to respond to antiangiogenic therapy in combination with chemotherapy, are not available.

To determine factors of importance for antiangiogenic treatment response and/or resistance, two representative human basal- and luminal-like breast cancer xenografts were treated with bevacizumab and doxorubicin alone or in combination. *In vivo* growth inhibition, microvessel density (MVD) and proliferating tumor vessels (pMVD = proliferative microvessel density) were analysed, while kinase activity was determined using the PamChip Tyrosine kinase microarray system.

Results showed that both doxorubicin and bevacizumab inhibited basal-like tumor growth significantly, but with a superior effect when given in combination. In contrast, doxorubicin inhibited luminal-like tumor growth most effectively, and with no additional benefit of adding antiangiogenic therapy. In agreement with the growth inhibition data, vascular characterization verified a more pronounced effect of the antiangiogenic treatment in the basal-like compared to the luminal-like tumors, demonstrating total inhibition of pMVD and a significant reduction in MVD at early time points (three days after treatment) and sustained inhibitory effects until the end of the experiment (day 18). In contrast, luminal-like tumors only showed significant effect on the vasculature at day 10 in the tumors having received both doxorubicin and bevacizumab.

Kinase activity profiling in both tumor models demonstrated that the most effective treatment *in vivo* was accompanied with increased phosphorylation of kinase substrates

Abbreviations: VEGF, Vascular Endothelial Growth Factor; OS, Overall survival; PFS, Progression free survival; CD31, Platelet Endothelial Cell Adhesion Molecule; MVD, Microvessel density; pMVD, proliferating MVD; PLCγ1, Phospholipase C gamma 1; EGFR, Epidermal Growth Factor Receptor; PDGFRβ, platelet-derived growth factor receptor beta; PR, Progesterone receptor; VEGFR2, Vascular Endothelial Growth Factor Receptor 2; ERK1/2, extracellular-signal-regulated kinases 1 and 2.

* *Corresponding author*. Tel.: +47 22 78 17 59; fax: +47 22 78 17 95.
E-mail addresses: Evita.Lindholm@rr-research.no, evilin@rr-research.no (E.M. Lindholm).

doi:10.1016/j.molonc.2012.03.006

of growth control and angiogenesis, like EGFR, VEGFR2 and PLCγ1. This may be a result of regulatory feedback mechanisms contributing to treatment resistance, and may suggest response markers of value for the prediction of antiangiogenic treatment efficacy.

1. Introduction

The formation of new blood vessels is an important property for the proliferation and expansion of solid tumors. Thus, targeting the angiogenic process represents a promising therapeutic approach, and several antiangiogenic drugs have been developed. VEGF-A (commonly referred to as VEGF) has been recognized as an important stimulator of angiogenesis, and its overexpression has been associated with tumor progression and poor prognosis in several tumor types, including breast cancer (Berns et al., 2003; Manders et al., 2002). Accordingly, treatment with the humanized monoclonal antibody bevacizumab, which binds and neutralizes all human VEGF-A isoforms, have shown increased overall (OS) and progression free survival (PFS) in patients with metastatic colorectal cancer when combined with first-line chemotherapy (Hurwitz et al., 2004). In breast cancer however, treatment with bevacizumab in combination with chemotherapy have been less successful. Variable improvements in PFS and no benefits in OS (Miles et al., 2010; Miller et al., 2007) have been observed, resulting in the FDA decision to withdraw the approval of bevacizumab as a treatment option for metastatic breast cancer.

However, the biological mechanisms responsible for treatment resistance are not fully understood. One explanation for the lack of an overall survival benefit may be that breast cancer is a clinically heterogeneous disease, with molecular subtypes responding differently to various treatments (Rouzier et al., 2005). A large clinical benefit in a small subpopulation of patients will be diluted in large clinical trials with unselected patients, and therefore, one of the most important challenges is to identify possible responders to different types of targeted therapies among the unselected group of breast cancer patients. In this regard, high baseline levels of VEGF-A in blood plasma of breast cancer patients has been found to correlate significantly with increased OS, and were of borderline significance ($p = 0.06$) with improved PFS following bevacizumab treatment (Jayson et al., 2011).Furthermore, Yang et al. demonstrated that patients with high expression of VEGF in the tumor cells, and CD31 and PDGFRβ in the tumor vasculature were more likely to respond to bevacizumab in combination with doxorubicin-docetaxel (Yang et al., 2008). Triple negative breast cancers (TNBC) are shown to have increased CD31 and VEGF expression (Linderholm et al., 2009), suggesting that this subtype of tumors could have a beneficial effect of antiangiogenic therapy. Accordingly, *in vivo* studies utilizing the triple negative breast cancer cell line MDA-MB-231 demonstrated that VEGF-A protected against chemotherapy, whereas the addition of bevacizumab sensitized the cells to paclitaxel-induced effects (Volk et al., 2008). This will be further studied in the BEATRICE phase III clinical trial, where bevacizumab will be added to standard adjuvant therapy in patients with TNBC. The effect of bevacizumab in the neoadjuvant setting is also currently under investigation in several randomized clinical trials, and recent studies have reported an increased fraction of pathological complete responses in the triple negative subset of patients treated with bevacizumab (von Minckwitz et al., 2012). However, in another recent clinical trial, the responding patients were found among the estrogen receptor positive patients (Bear et al., 2012), thus emphasizing the need for further research to identify the patient population responding to antiangiogenic therapy.

In the current project we used two ortothopic xenograft models, representing luminal-like (hormone receptor positive) and basal-like (triple negative) breast cancers, to study the effects of antiangiogenic therapy and chemotherapy. The effects on tumor growth were compared with changes induced in the tumor vasculature and at the molecular level in the harvested tumor material. Such analyses may define pathways involved in treatment response or development of resistance, as well as possible molecular targets to be exploited as biomarkers for prediction of therapy response.

2. Materials and methods

2.1. Animal models and treatments

Two breast cancer xenograft models, MAS98.06 and MAS98.12, derived from primary mammary adenocarcinoma specimens (MAS) have previously been described (Bergamaschi et al., 2009). Molecular characterization of the two xenografts has classified MAS98.06 as luminal-like and hormone receptor positive, while MAS98.12 has been classified as basal-like and hormone receptor negative. Locally bred athymic nude mice (NCr-Foxn1^{nu}) were kept under pathogen-free conditions, at constant temperature (21.5 ± 0.5 °C) and humidity (55 ± 5%), 20 air changes/hr and a 12 h light/dark cycle. Small pockets were created in the mammary fat pads, wherein tumor pieces of 1–2 mm^3 were implanted. Distilled tap water was given *ad libitum*, and was supplemented with 17-β-estradiol at a concentration of 4 mg/L. The latter was done to ensure growth of the MAS98.06 xenograft, which is dependent on estrogen. The mice were randomly assigned into the following treatment groups after the tumor diameter reached approximately 5 mm; controls, bevacizumab treatment (5 mg/kg, intraperitonealy (I.P.)) given twice weekly, doxorubicin treatment (8 mg/kg intravenously (I.V.)) given once at the start of the experiment, and one group of animals receiving a combination of both treatments. Tumor growth was measured twice weekly, and tumor volumes were calculated using the formula length × width × width × 0.5. In each treatment group the animals were sacrificed and tumor tissue harvested

at day 3, 10 or at symptom onset in control mice. Two independent experiments were performed in the basal-like and luminal-like tumor models, with the total number of luminal-like tumors being 36, 43 and 58 for day 3, 10 and 35 respectively, and the total number of basal-like tumors being 44, 44 and 49 for day 3, 10 and 18 respectively. Tumor tissue from both experiments was stored in liquid nitrogen for protein phosphorylation analysis, and was fixed in 10% buffered formalin for 48 h for analyses by immunohistochemistry. All procedures and experiments involving animals were approved by The National Animal Research Authority, and were conducted according to the European Convention for the Protection of Vertebrates used for Scientific Purposes. All procedures and endpoints were in compliance with what has previously been described (Workman et al., 2010).

2.2. Histopathology

A middle section from each tumor at the three different time points was fixed in 10% buffered formalin phosphate for immunohistochemistry analysis. A total of seven tumors from each treatment group were analysed, from the two independent studies. A sequential dual staining using the proliferation marker Ki-67 rat anti-mouse antibody (Dako Cambridge, UK; M7249, Clone TEC 3, dilution 1:50) and the pan-endothelial marker CD34 rat anti-mouse antibody (Abcam, Cambridge, UK; Clone MEC 14.7 dilution 1:50) were applied. After Ki-67 staining, the sections were incubated with an alkaline phosphatase-conjugated secondary goat anti-rat antibody (Santa Cruz Biotechnology, CA, USA; sc-3824, dilution 1:100, 60 min), followed by Ferangi blue chromogen kit (Biocare Medical, Walnut Creek, CA, USA) applied for 20 min. After rinsing in buffer and denaturation solution (Biocare Medical), CD34 rat anti-mouse antibody was applied, followed by incubation with a HRP-conjugated secondary goat anti-rat antibody (Santa Cruz; sc-3823, dilution 1:50, 30 min). AEC + substrate chromogen (Dako) was then applied for 20 min and sections were finally rinsed in distilled water and mounted. No contrast staining was applied.

Before counting of microvessel density (MVD), an examination at low magnification was performed to identify the most vascular areas in the tumor sections; 10 fields (×250, 0.424 mm^2) were examined, and the counts of positively stained vessels were expressed per area examined (counts/mm^2). The proliferating endothelial cells were recognized by their morphology, localization and their combined Ki-67 and CD34 staining.

2.3. Tyrosine kinase activity profiling by PamChip peptide arrays

Kinase activity profiles were carried out using the PamChip Tyrosine Kinase Microarray System (PamGene, The Netherlands). This microarray contains 144 phospho-peptides immobilized on a porous membrane, where each peptide represents a sequence corresponding to a specific tyrosine kinase substrate. The tumor lysates are pulsed through the porous material, which allows rapid phosphorylation of the peptide sequences by active kinases in the lysate. Thus the technique allows functional comparison of active signaling pathways in different biological samples, by measuring the level of kinase activity.

Tissue used for the PamGene analysis was from three tumors in each treatment group, all belonging to one of the two individual experiments. Tumor tissue was from passage 47 for MAS98.12 and passage 28 for MAS98.06. To avoid freezing-thawing cycles prior to analysis, frozen tumors from MAS98.06 and MAS98.12 xenografts were cut in 10 μm slices to a total of 1.4 mm^3 tissue. Addition of 50 μl M-PER Mammalian Protein Extract Reagent (Pierce, Rockford, IL, USA), supplemented with 1% Halt Protease Inhibitor Cocktail, EDTA-free (Pierce) and 1% Halt Phosphatase Inhibitor Cocktail (Pierce), to this amount of tissue, gives a protein lysate of approximately 1 μg/μl. Before loading of lysate, each array was blocked with 20 μg/ml bovine serum albumin (BSA). Next, 5 μl lysate was loaded onto plates in a mixture consisting 1× ABL buffer (50 mM Tris–HCl pH 7.5, 10 mM $MgCl_2$, 1 mM EGTA, 2 mM dithiothreitol, 0.01% Brij 35 (New England BioLabs, Inc., Ipswich, MA)), 1 mg/ml BSA, 100 μM ATP (Sigma-Aldrich) and 12.5 μg/ml FITC conjugated monoclonal anti-phospho-tyrosine antibody (PY20, Exalpha Biologicals, Maynard, MA, USA). Three tumors from each treatment group were analyzed. Each biological sample was run in four technical replicates, and for every fifth pump cycle a 16-bit TIFF image was taken with a built-in CCD camera.

2.4. Western immunoblot analysis

To confirm the data obtained by the PamChip kinase substrate arrays, lysate from the same tumors as used for the pamgene analysis was analysed on western immunoblots. Membranes were probed with phospho-specific antibodies against the same phospho-tyrosine that turned out significant on the corresponding substrate in the PamChip array (Supplementary Table 1), followed by peroxidase-conjugated secondary antibodies. Proteins were visualized using a SuperSignal West Dura Luminol/Enhancer solution (Pierce, Rockford, IL), and membranes were exposed to Kodak X-ray films for 1–5 min before developing.

2.5. Data analysis and statistics

In vivo growth curves were generated from mean relative tumor volumes. Statistical significance of treatment effect was assessed by taking the slope intercept at all time points, and calculate statistical difference with $P < 0.05$ (Student's *t*-test).

The SigmaPlot statistical package (Systat Software Inc, San Jose, CA) was used to analyse the association between mean MVD or pMVD values in different treatment groups. Mann–Whitney *U* test was performed, and differences were considered to be significant for values of $P < 0.05$.

Data from the PamGene kinome profiling was linked to peptide identities using EVOLVE PAMGRID software, and quantification of spot intensities was conducted using Bionavigator software (PamGene International BV). Replicates from visually damaged wells were removed from the analysis. Due to the lack of available plate-to-plate standardization, only samples analyzed on the same plate were compared. Data normalization was achieved by determining the median signal intensity for individual peptides on the PamChip.

Treatment effects were assessed by fitting an ANOVA model to the signal intensities using treatment and individual as explanatory factors. Benjamini and Hochberg (1995) false discovery rates (FDR) were calculated from the p-values for the treatment effects. Peptides with FDR smaller than 10% were considered significant.

Individual bands from western immunoblots were quantified by densitometric measurements and mean fold changes relative to loading control (α-tubulin or β-actin) was calculated with a statistical difference of $P < 0.05$ (Student's t-test).

3. Results

3.1. *Effects of antiangiogenic treatment in orthotopic breast cancer xenografts*

Mice inoculated with the basal-like (MAS98.12) or the luminal-like (MAS98.06) breast cancer xenografts were treated with bevacizumab, doxorubicin or a combination of both, for three and ten days, or until control mice had to be sacrificed at day 18 (basal)/day 35 (luminal). Growth curves were generated from the latter groups of mice (Figure 1).

In basal-like tumors, all treatment regimens reduced the growth significantly ($p < 0.01$) when compared to controls, with a maximal growth inhibition in tumors treated with the combination ($p < 0.001$). In addition, the combination treatment was significantly better than both doxorubicin ($p = 0.01$) and bevacizumab ($p < 0.01$) monotherapies. In contrast, the luminal-like breast cancer xenografts demonstrated a superior response to the doxorubicin containing regimen ($p < 0.01$), whereas bevacizumab monotherapy only reduced the tumor growth with borderline significance compared to the control group ($p = 0.053$). No additional effect was seen in xenografts treated with doxorubicin in combination with bevacizumab, compared to doxorubicin alone ($p = 0.37$).

3.2. *Characterization of tumor vasculature*

Treatment with bevacizumab monotherapy significantly reduced the number of tumor associated capillaries (MVD) both three and ten days after start of treatment in the basal-like tumors (Table 1). A similar decrease in proliferating endothelial cells (pMVD) was also demonstrated after this treatment, but with a borderline significance ($p = 0.051$) at day 10. Combination treatment exhibited similar results as bevacizumab, with a significant (or borderline significant in the case of MVD at day 3) decrease in MVD and pMVD at both day 3 and 10.

At the end of the experiment (after approximately three weeks), MVD and pMVD was still reduced in the bevacizumab treated tumors, but without statistical significance. However, in the combination treated tumors MVD was still significantly lower when compared to doxorubicin treated tumors, indicating the superior effect of combination therapy, compared to antiangiogenic monotherapy.

In the luminal-like tumors, no significant effect on the vasculature was seen in any of the treatment regimens at day 3. However, at day 10 the tumors treated with combination therapy demonstrated significantly reduced MVD and pMVD values. At this time point MVD was also found reduced ($p = 0.054$) after doxorubicin monotherapy. The effects on MVD and pMVD were temporary, as no significant reduction was found at the end of the experiment.

3.3. *Therapy-induced changes in kinase activity in the basal-like tumors*

To investigate if the antiangiogenic effects observed *in vivo* were related to any changes at the molecular level, analysis of kinase activity three and ten days after treatment was carried out using the PamChip kinase activity profiling platform.

Interestingly, the results revealed similar response patterns in the two tumor models, in relation to the most effective treatment *in vivo*, that is, combination treatment in the basal-like (Table 2) and doxorubicin treatment in the luminal-like (Supplementary Table 5).

The basal-like xenografts were more responsive to antiangiogenic therapy when evaluating *in vivo* growth inhibition and according to the vasculature characterization, compared to the luminal-like. Kinase activity profiling three days after bevacizumab treatment revealed a significant increase in the phosphorylation of several kinase substrates ($n = 73$,

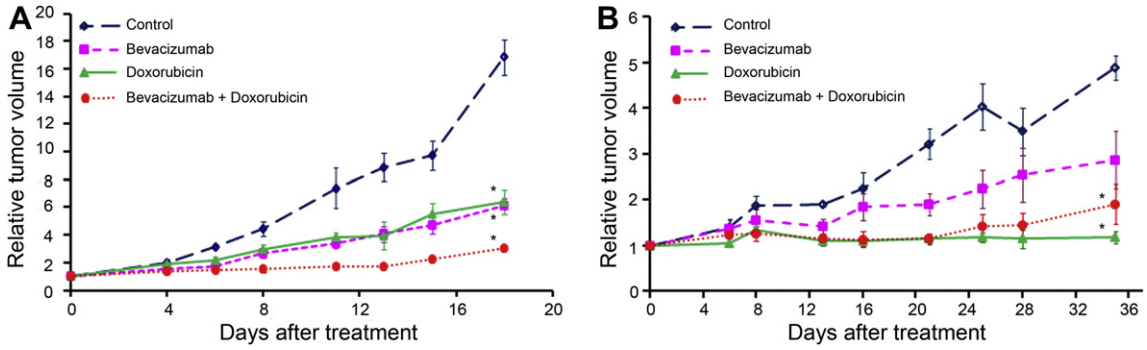

Figure 1 – Growth curves showing *in vivo* inhibition of basal-like (A) and luminal-like (B) xenografts by treatment with bevacizumab, doxorubicin, and the combination. Significant inhibition (*) of basal-like tumor growth was seen in all treatments groups ($p < 0.01$), with a superior result in mice receiving the combination treatment, both compared to controls ($p < 0.01$) and monotherapy treated tumors ($p < 0.01$ for bevacizumab and $p = 0.01$ for doxorubicin). In contrast, doxorubicin treatment resulted in most significant tumor inhibition in the luminal-like breast cancer tumors ($p < 0.01$), without any statistically significant improvement with the addition of bevacizumab ($p = 0.37$). Error bars indicate ±SEM.

Table 1 – Effects on vasculature (MVD and pMVD) in basal-like and luminal-like breast cancer xenografts after treatment with bevacizumab, doxorubicin and a combination of both.

	Treatment for three days				Treatment for ten days				End of experiment[b]			
	MVD[a]	P[c]	pMVD[a]	P[c]	MVD[a]	P[c]	pMVD[a]	P[c]	MVD[a]	P[c]	pMVD[a]	P[c]
Basal-like												
Control	69.0	–	1.4	–	68.6	–	2.1	–	39.1	–	0.9	–
Bevacizumab	30.5	0.015	0.0	0.009	21.3	0.001	0.9	0.051	39.6	–	0.4	–
Doxorubicin	52.0	–	0.4	–	59.3	–	1.3	–	62.7	–	1.1	–
Bevacizumab + Doxorubicin	11.6	0.051	0	0.001	24.7	0.001	0.7	0.014	35.8	–	0.2	–
Combination vs Doxorubicin		–		0.004		0.001		–		0.026		
Luminal-like												
Control	56.9	–	1.0	–	60.0	–	0.9	–	28.7	–	0.8	–
Bevacizumab	38.9	–	0.7	–	45.3	–	0.2	–	44.3	–	0.7	–
Doxorubicin	44.5	–	0.4	–	51.4	0.054	0.2	–	29.6	–	0.8	–
Bevacizumab + Doxorubicin	46.3	–	0.8	–	32.2	0.026	0.0	0.011	36.1	–	0.4	–
Combination vs Doxorubicin		–		–		<0.001		–		–		–

- : $p > 0.05$.
a Median values.
b Day 18 for basal-like, day 35 for luminal-like.
c Mann–Whitney U test.

Supplementary Table 2), where many of them are involved in angiogenesis and growth control. However, this effect was short lived as only a few kinase substrates ($n = 23$) were found affected at day 10 (Supplementary Table 2), and in contrast to day 3 they were phosphorylated to a lesser extent than in the control tumors.

Doxorubicin monotherapy demonstrated similar growth inhibitory effects as single agent bevacizumab *in vivo*, and interestingly, the treatment associated changes in kinase activity were also similar. That is, doxorubicin treatment also resulted in upregulated phosphorylation of several kinase substrates ($n = 71$) compared to non-treated tumors at day 3, followed by a decrease ($n = 25$) at day 10 (Supplementary Table 3).

Although doxorubicin and bevacizumab significantly reduced the *in vivo* growth rate in the basal-like tumors when administrated alone, the combination treatment resulted in significantly increased efficacy. Interestingly, while the monotherapy regimens demonstrated a reduction in kinase activity at day 10, the combination treatment resulted in increased kinase activity ($n = 45$) at this time point (Table 2). Among the upregulated kinase substrates, many are known to be important in pathways stimulating tumor growth and angiogenesis, i.e. epidermal growth factor receptor (EGFR), platelet-derived growth factor beta (PDGFRB) and VEGFR2. In the latter analysis combination therapy was compared to doxorubicin in attempt to define markers responsible for the additional growth inhibitory effect observed when adding bevacizumab to traditional chemotherapy. Results showed that many of the kinase substrates that were only found in the combination treated tumors at day 10 uses phospholipase C-gamma 1 (PLCγ1) as a downstream signaling protein, suggesting an important role for this protein in sustained tumor growth.

3.4. *Therapy-induced changes in kinase activity in the luminal-like tumors*

Kinase activity profiling of bevacizumab treated luminal-like tumors demonstrated a downregulation of substrate phosphorylation in treated compared to control tumors at day 3 ($n = 77$), and without any significant change in any substrates at day 10 ($n = 0$, Supplementary Table 4). On the contrary, doxorubicin monotherapy, which showed the highest growth inhibitory efficacy in luminal-like tumors *in vivo*, demonstrated a high level of treatment associated changes in kinase activity; Small changes in phosphorylation in a few substrates was observed at day 3 ($n = 16$), while a significant and marked phosphorylation of several additional substrates were detected on day 10 ($n = 84$, Supplementary Table 5).

Due to the superior growth inhibitory effects of doxorubicin monotherapy in the luminal-like tumors, any additional effects of adding bevacizumab may be difficult to distinguish. Accordingly, kinase activity profiling demonstrated that combination versus doxorubicin treatment resulted in similar phosphorylation patterns as bevacizumab monotherapy, with a small degree of decrease at day 3 (Supplementary Table 6) followed by a normalization at day 10 (Table 2). This is in significant contrast to the bevacizumab response seen in the basal-like tumors (Table 2), highlighting the biological differences in response to antiangiogenic therapy.

3.5. *Validation of protein tyrosine phosphorylation by western immunoblotting*

The PamChip kinase activity profiling technology is relatively new. Furthermore, the kinase substrates are peptides consisting of 13–14 amino acids, which may have similarities with other substrates, and cross-reactivity cannot be excluded. We therefore validated some of the PamGene results by western immunoblotting with phospho-specific antibodies (Supplementary Table 1).

Bevacizumab targets VEGF-A and therapy with this agent is therefore thought to influence on the Vascular Endothelial Growth Factor Receptor 2 (VEGFR2) activity. The PamGene analysis indicated a 1.47 fold increase in phosphorylation on $Tyr^{1054/1059}$ in VEGFR2 three days after the first bevacizumab injection in mice with basal-like tumors. Furthermore, the

Table 2 – Fold changes in kinase activity in basal- and luminal-like xenografts, ten days after combination relative to doxorubicin treatment. Bevacizumab + Doxorubicin/Doxorubicin.

Kinase substrate	Swiss Prot ID	Basal-like	Luminal-like	PLCγ1[a]
ACHD_Y383/Y390	Q07001	1.27	–	
ANXA2_Y24	P07355	1.18	–	
CD3Z_Y123	P20963	1.25	–	(Nel et al., 1995)
CDK2_Y15/Y19	P24941	1.40	–	
CTNB1_Y86	P35222	1.22	–	
DCX_Y112	O43602	1.20	–	
DDR1_Y513	Q08345	1.76	1.28	
EGFR_Y1110	P00533	1.28	–	(Xie et al., 2010a; Xie et al., 2010b)
EPHA2_Y772	P29317	1.35	–	
EPHA7_Y608/Y614	Q15375	1.13	–	
EPHB1_Y778	P54762	1.23	–	
EPOR_Y368	P19235	1.32	–	(Marrero et al., 1998; Ren et al., 1994)
EPOR_Y426	P19235	1.26	–	
FER_Y714	P16591	1.23	–	
FES_Y713	P07332	1.41	–	
FRK_Y387	P42685	1.39	–	
JAK1_Y1022/Y1023	P23458	1.16	–	
JAK2_Y570	O60674	1.17	–	
K2C6B_Y62	P04259	1.14	–	
LCK_Y394	P06239	1.18	–	(Weber et al., 1992)
MBP_Y261/Y268	P02686	1.17	–	
MBP_Y268	P02686	1.19	–	
MET_Y1230/Y1234/Y1235	P08581	1.18	–	(Machide et al., 2000)
MK01_Y187	P28482	1.24	–	(Yang et al., 2001)
MK07_Y215/Y220	Q13164	1.14	–	
MK12_Y185	P53778	1.27	–	
PAXI_Y31/Y33	P49023	1.28	–	(Chang et al., 1999)
PDGFRB_Y1021	P09619	1.10	–	(Poulin et al., 2000)
PDGFRB_Y579/Y581	P09619	1.17	–	
PDGFRB_Y771/Y775/Y778	P09619	1.31	–	
PLCG1_Y771/Y775	P19174	1.25	–	
PR_Y795	P06401	1.26	–	
RAF1_Y340/Y341	P04049	1.23	–	(Yang et al., 2001)
RASA1_Y460	P20936	1.32	–	
RET_Y1029	P07949	1.31	–	(Borrello et al., 1996; Mason, 2000)
RON_Y1353/Y1360	Q04912	1.26	–	(Iwama et al., 1996)
SRC8_CHICK_Y477/Y483	Q01406	1.18	–	
STAT4_Y725	Q14765	1.32	–	
TEC_Y513/Y519	P42680	1.16	–	(Tomlinson et al., 2004)
TYRO3_Y681/Y685/Y686	Q06418	1.21	–	
VEGFR1_Y1327/Y1333	P17948	1.17	–	(Ito et al., 1998)
VEGFR2_Y951	P35968	1.19	–	
VEGFR2_Y996	P35968	1.47	–	
VINC_Y822	P18206	1.22	–	
ZAP70_Y492/Y493	P43403	1.27	–	(Williams et al., 1999)

All values are estimated with $p < 0.05$ and cut-off at 10%.
a Reference coupling kinase substrate to PLCγ1 signaling.

Tyr[996] site on the same receptor was upregulated with the same magnitude in combination treated basal-like tumors at day 10, compared to the doxorubicin treated tumors. Immunoblotting with antibodies directed against these epitopes confirmed a clear upregulation of the VEGFR2 phosphorylation in the treated tumors, as indicated in Figure 2A and D.

Enhanced expression and activity of EGFR has been associated with a number of cancers, including breast cancer, while Annexin A2 has been linked to enhanced invasion in several cancer types. The PamGene results indicated over two-fold increase in phosphorylation of the Tyr[1197] site in EGFR and the Tyr[24] site in Annexin A2, three days after treatment of the basal-like tumors with either bevacizumab or doxorubicin monotherapy. As demonstrated in Figure 2(B and C) the immunoblotting results confirmed these changes in bevacizumab treated tumors.

For many of the kinases the activity of which were found upregulated at day 10 in combination versus doxorubicin treated basal-like tumors signal, among others, through PLCγ1, and the Pamgene analysis suggested a 1.25 fold

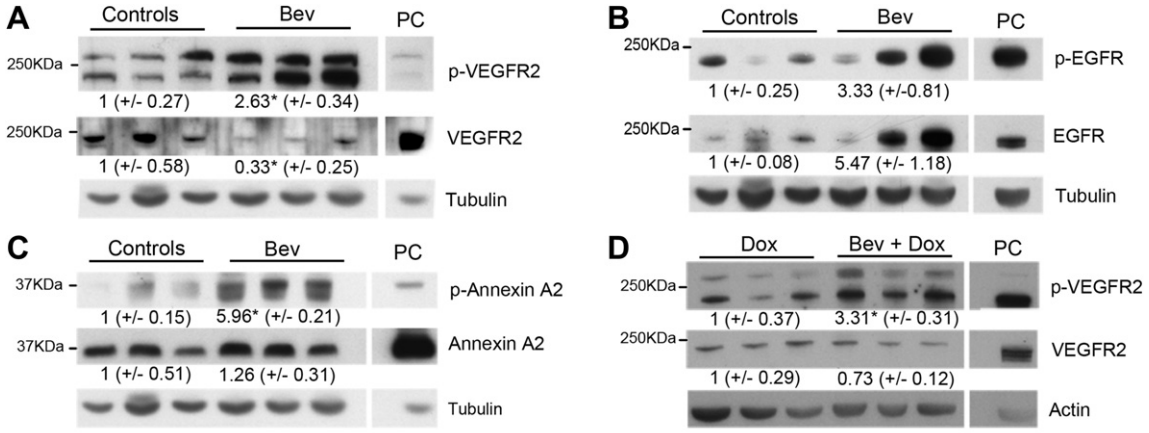

Figure 2 – Immunoblotting of proteins isolated from the basal-like tumors three days after bevacizumab treatment (A, B and C), or ten days after bevacizumab and doxorubicin combination treatment (D). Antibodies against phosphorylated VEGFR2 Tyr$^{1054/1059}$, EGFR Tyr^{1197} and Annexin A2 Tyr^{24} (A, B and C, respectively) confirmed enhanced phosphorylation in bevacizumab treated tumors, compared to controls. In panel *D* increased VEGFR2 Tyr^{996} phosphorylation is confirmed in the combination compared to doxorubicin treated tumors at day 10. HUVEC cells were used as positive control (PC) for pVEGFR2, while MDA-MB-231 cells were used as PC for pEGFR and p-ANNEXIN A2. Values indicate mean protein concentration, as quantified by densitometric measurements, ±SEM. $^{*}p < 0.05$.

increase in phosphorylation of Tyr$^{771/775}$ in PLCγ1 at day 10. This was confirmed by immunoblotting with an antibody targeting Tyr^{771}, in addition to a pan PLCγ1 antibody (Figure 3A). To investigate further downstream signaling pathways, antibodies targeting phosphorylated and total ERK1/2 and Akt were used. Immunoblotting revealed upregulation of phosphorylated ERK1/2 in combination versus doxorubicin treated basal-like tumors at day 10 (Figure 3B), which is also in agreement with the ERK2 Tyr^{187} upregulation found by the PamGene analysis at this time point (Table 2). In contrast, a downregulation of phosphorylated and total Akt was found in combination versus doxorubicin treated basal-like tumors, indicating a downregulation of this protein upon bevacizumab addition to doxorubicin.

Some variability within treatment groups was observed, as expected in biological replicates. However, densitometric measurements confirmed the results found in the Pamgene analyses.

4. Discussion

In this paper we have demonstrated that the fast growing basal-like and the slower growing luminal-like breast cancer models responded differently to antiangiogenic treatment in combination with chemotherapy *in vivo*. The differences were also verified at the molecular level, showing that the most effective therapy for each tumor type elicited a marked upregulation in signaling activity. Tumor growth curves indicated a beneficial effect of antiangiogenic treatment in the basal-like breast cancer xenograft, with the combination of bevacizumab and doxorubicin as the most effective therapy. In contrast, doxorubicin monotherapy was highly efficient in the luminal-like model, with no significant benefit obtained by adding bevacizumab. These results are in line with previous reports indicating that an appropriate selection of patients with specific tumor characteristics is needed for an efficient use of antiangiogenic therapy.

Clinical trials with bevacizumab in breast cancer patients have shown various effects. However, in the metastatic setting, chemotherapy in combination with antiangiogenic therapy has been found superior compared to chemotherapy alone, although the magnitude of benefit has been questioned (Miles et al., 2010; Miller et al., 2007). This is in agreement with our present findings, indicating that the basal-like xenografts responded better to combination therapy than to monotherapy with either doxorubicin or bevacizumab. Several studies have proposed that the observed effect is a consequence of tumor vessel normalization, which results in decreased interstitial pressure and thereby more efficient chemotherapy delivery (Jain, 2005). Recent studies of human breast cancer xenografts support this view, demonstrating increased paclitaxel concentrations and improved permeability after bevacizumab treatment (Yanagisawa et al., 2010).

Both the basal-like and luminal-like xenografts responded with a significant decrease in endothelial proliferation upon combination therapy. This effect was more pronounced in the basal-like xenografts with a significantly reduced MVD three days after bevacizumab monotherapy, and (borderline significance) after combination therapy. The decrease in MVD persisted for approximately three weeks in the tumors treated with the combination, and was statistically significant when compared to the doxorubicin treated xenografts. These data support the *in vivo* growth curves and previous studies demonstrating a more pronounced effect of antiangiogenic treatment in tumors with basal-like characteristics. We hypothesize that the lack of significantly reduced MVD values in the luminal-like tumors at day 3 is due to an insufficient duration of the treatment in this slower growing tumor. This hypothesis was further strengthened by the significant decrease in MVD and pMVD after ten days of combination treatment. At this time point a borderline significant decrease in MVD was also found in doxorubicin treated tumors.

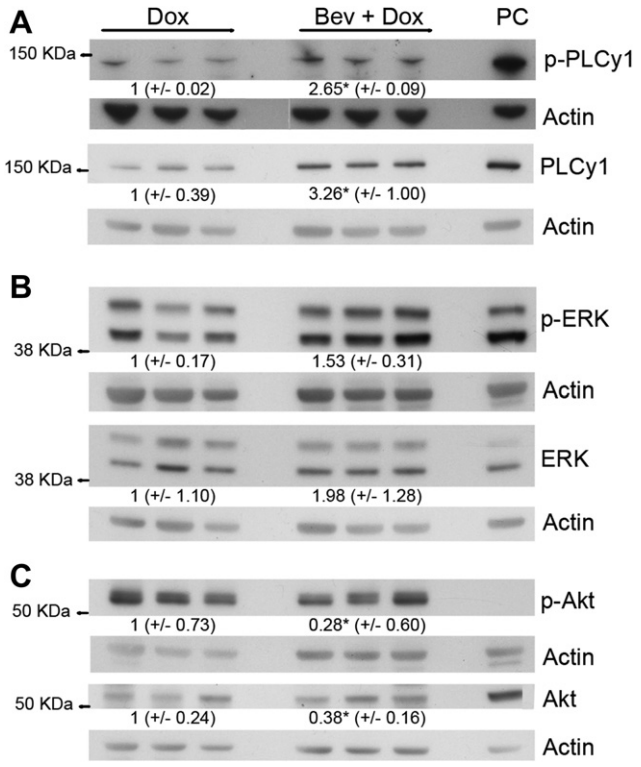

Figure 3 – Immunoblotting of proteins isolated from the basal-like tumors ten days after doxorubicin and combination treatment. Antibodies against phosphorylated PLCγ1 Tyr^{771} (A) and ERK Thr^{202}/Tyr^{204} (B) confirmed the increased signaling in combination treated tumors, compared to doxorubicin monotherapy. In contrast, Akt Ser^{473} was shown to be downregulated. MDA-MB-231 cells were used as positive control (PC). Values indicate mean protein concentration, as quantified by densitometric measurements, ±SEM. $^{*}p < 0.05$.

As measured by IHC, none of the endothelial proliferation markers were significantly reduced at the end of the experiment. These results are in line with clinical observations, where initial responses to both chemotherapeutic and antiangiogenic treatments often are short lived and followed by recurrent tumor growth due to acquired resistance. This may be explained through upregulation of compensatory feedback mechanisms, enabling the tumor to escape anti-VEGF therapy by exploiting other alternative pro-angiogenic factors to stimulate the tumor vasculature. This emphasizes the need for a longitudinal characterization of the angiogenic process, in order to get a better understanding of molecular mechanisms underlying intrinsic or acquired resistance, and possibly identify potential targets when the tumor evolves resistance. However, the lack of sustained effects may also be due to loss of doxorubicin-induced responses in the combination treated groups, as this treatment was only given once at the start of the experiment. This regimen was chosen due to the similarity of clinical scheduling, where doxorubicin is administered every third week.

The results from the tumor vasculature analysis are important as they show that antiangiogenic therapy with bevacizumab do indeed exhibit a biologic effect in both tumor types. However, a marked early inhibition of vascular proliferation seemed to associate with a sustained antitumor response *in vivo*, as demonstrated for the basal-like, but not the luminal-like, xenografts.

Identification of markers of antiangiogenic response, or the lack of such, in different breast cancer subtypes is highly warranted. In this study we utilized the PamChip kinase profiling technology to identify signaling pathways affected by antiangiogenic treatment *in vivo*. The kinase activity profile after antiangiogenic therapy with bevacizumab was different in basal-like and luminal-like tumors, further demonstrating the difference in antiangiogenic response between these two subtypes of breast cancer. Basal-like tumors responded with a strong upregulation in kinase activity three days after bevacizumab and doxorubicin monotherapies, followed by a weaker downregulation on day 10. However, the addition of doxorubicin to bevacizumab resulted in increased kinase activity at both time points. In contrast, bevacizumab monotherapy showed no effect on kinase activity at day 10 in the luminal-like tumors, whereas doxorubicin monotherapy resembled the high kinase activity pattern found in the combination treated basal-like tumors. The lack of kinase activity response after bevacizumab treatment in the luminal-like tumors at day 10, corresponded to the low antiangiogenic effects demonstrated both *in vivo* and in the vascular markers. Interestingly, the phosphorylation analyses performed on the basal- and luminal-like tumors demonstrated similar responses at the molecular level; the treatment causing the most significant growth inhibition *in vivo* was accompanied with a higher level of kinase activity at day 10. The obtained results indicated that several pathways are "turned on" following effective growth inhibitory treatment, which may indicate compensatory mechanisms and thus possible targets for treatment resistance. Further studies are needed and are ongoing to define upregulated proteins as "drivers" or "passengers", but the trend gives valuable information about the molecular defence mechanism that are activated to overcome a treatment effect.

One of the substrates found with enhanced level of phosphorylation in combination versus doxorubicin treated basal-like tumors at day 10 was PLCγ1, and several of the other upregulated substrates also utilize this protein for downstream signaling. PLCγ1 is highly expressed in several tumors, including breast carcinomas (Arteaga et al., 1991), and has been shown to play a critical role in cell survival, proliferation and metastasis (Markova et al., 2010; Sala et al., 2008), in addition to angiogenesis (Husain et al., 2010) and vascular permeability (Pocock and Bates, 2001). The findings presented here therefore support earlier reports introducing this enzyme as a possible candidate for targeted therapy (Kassis et al., 1999; Markova et al., 2010). However, it is unlikely that the effect from a number of important regulators of tumor proliferation and aggressiveness can be counteracted by the inhibition of one enzyme. Therefore, simultaneous inhibition of a number of these targets and alternative pathways may be needed to overcome treatment resistance.

In conclusion, our study demonstrated different growth inhibitory efficacy and molecular responses in the two breast cancer subtypes, with clear improvements in basal-like treatment effects when adding bevacizumab to doxorubicin. Importantly, an early reduction in endothelial proliferation

may suggest a clinical meaningful response on tumor growth in this subtype of breast cancer. In addition, potential signaling pathways identified by kinase activity profiling may suggest candidate markers for selection of patients for antiangiogenic therapy, and for identifying targets to combat treatment related resistance. To our knowledge this is the first paper analysing the proteomic effects of bevacizumab treatment in different breast cancer subtypes, at different time points and in combination with chemotherapy. This will be exploited further in an ongoing neoadjuvant clinical trial (ClinicalTrials.gov: NCT00773695).

Ethical approval

The authors declare that all experiments followed the ethical guidelines in Norway and the EU. All procedures and experiments involving animals were approved by The National Animal Research Authority, and were conducted according to the European Convention for the Protection of Vertebrates used for Scientific Purposes; as stated in Materials and methods.

Acknowledgement

This work was supported from the National Program for Functional Genomics, the Research Council of Norway (project no: 183621/S10), the South-Eastern Norway Regional Health Authority and the Norwegian Cancer Society (project number 421852). Olav Engebraaten was supported by a gift from late Monica Nordals relatives.

The authors are grateful to Eldrid Borgan for help on statistical calculations, and to Gerd Lillian Hallseth and Bendik Nordanger for excellent technical help.

Appendix A. Supplementary material

Supplementary material associated with this article can be found, in the online version, at doi:10.1016/j.molonc.2012.03.006.

REFERENCES

Arteaga, C.L., Johnson, M.D., Todderud, G., Coffey, R.J., Carpenter, G., Page, D.L., 1991. Elevated content of the tyrosine kinase substrate phospholipase C-gamma 1 in primary human breast carcinomas. Proceedings of the National Academy of Sciences of the United States of America 88, 10435–10439.

Bear, H.D., Tang, G., Rastogi, P., Geyer, C.E., Robidoux, A., Atkins, J.N., Baez-Diaz, L., Brufsky, A.M., Mehta, R.S., Fehrenbacher, L., Young, J.A., Senecal, F.M., Gaur, R., Margolese, R.G., Adams, P.T., Gross, H.M., Costantino, J.P., Swain, S.M., Mamounas, E.P., Wolmark, N., 2012. Bevacizumab added to neoadjuvant chemotherapy for breast cancer. New England Journal of Medicine 366, 310–320.

Benjamini, Y., Hochberg, Y., 1995. Controlling the false discovery rate: a practical and powerful approach to multiple testing. Journal of the Royal Statistical Society 57, 289–300.

Bergamaschi, A., Hjortland, G.O., Triulzi, T., Sorlie, T., Johnsen, H., Ree, A.H., Russnes, H.G., Tronnes, S., Maelandsmo, G.M., Fodstad, O., Borresen-Dale, A.L., Engebraaten, O., 2009. Molecular profiling and characterization of luminal-like and basal-like in vivo breast cancer xenograft models. Molecular Oncology 3, 469–482.

Berns, E.M., Klijn, J.G., Look, M.P., Grebenchtchikov, N., Vossen, R., Peters, H., Geurts-Moespot, A., Portengen, H., van Staveren, I.L., Meijer-van Gelder, M.E., Bakker, B., Sweep, F.C., Foekens, J.A., 2003. Combined vascular endothelial growth factor and TP53 status predicts poor response to tamoxifen therapy in estrogen receptor-positive advanced breast cancer. Clinical Cancer Research 9, 1253–1258.

Borrello, M.G., Alberti, L., Arighi, E., Bongarzone, I., Battistini, C., Bardelli, A., Pasini, B., Piutti, C., Rizzetti, M.G., Mondellini, P., Radice, M.T., Pierotti, M.A., 1996. The full oncogenic activity of Ret/ptc2 depends on tyrosine 539, a docking site for phospholipase Cgamma. Molecular and Cellular Biology 16, 2151–2163.

Chang, J.-S., Iwashita, S., Lee, Y.H., Kim, M.J., Ryu, S.H., Suh P-, G., 1999. Transformation of rat fibroblasts by phospholipase C-γ1 overexpression is accompanied by tyrosine dephosphorylation of paxillin. FEBS Letters 460, 161–165.

Hurwitz, H., Fehrenbacher, L., Novotny, W., Cartwright, T., Hainsworth, J., Heim, W., Berlin, J., Baron, A., Griffing, S., Holmgren, E., Ferrara, N., Fyfe, G., Rogers, B., Ross, R., Kabbinavar, F., 2004. Bevacizumab plus irinotecan, fluorouracil, and leucovorin for metastatic colorectal cancer. The New England Journal of Medicine 350, 2335–2342.

Husain, D., Meyer, R., Mehta, M., Pfeifer, W.M., Chou, E., Navruzbekov, G., Ahmed, E., Rahimi, N., 2010. Role of c-Cbl dependent regulation of phospholipase C gamma 1 activation in Experimental Choroidal Neovascularization. Investigative Ophthalmology & Visual Science 51, 6803–6809.

Ito, N., Wernstedt, C., Engstrom, U., Claesson-Welsh, L., 1998. Identification of vascular endothelial growth factor receptor-1 tyrosine phosphorylation sites and binding of SH2 domain-containing molecules. The Journal of Biological Chemistry 273, 23410–23418.

Iwama, A., Yamaguchi, N., Suda, T., 1996. STK/RON receptor tyrosine kinase mediates both apoptotic and growth signals via the multifunctional docking site conserved among the HGF receptor family. The EMBO Journal 15, 5866–5875.

Jain, R.K., 2005. Normalization of tumor vasculature: an emerging concept in antiangiogenic therapy. Science 307, 58–62. New York, NY.

Jayson, G.C., Haas, Sd, Delmar, P., Miles, D.W., Shah, M.A., Cutsem, E.V., Carmeliet, P., Hegde, P., Wild, N., Scherer, S.J., 2011. Evaluation of plasma VEGFA as a potential predictive pan-tumour biomarker for bevacizumab. 2011 European Multidisciplinary Cancer Congress Abstract 804

Kassis, J., Moellinger, J., Lo, H., Greenberg, N.M., Kim, H.G., Wells, A., 1999. A role for phospholipase C-gamma-mediated signaling in tumor cell invasion. Clinical Cancer Research 5, 2251–2260.

Linderholm, B.K., Hellborg, H., Johansson, U., Elmberger, G., Skoog, L., Lehtio, J., Lewensohn, R., 2009. Significantly higher levels of vascular endothelial growth factor (VEGF) and shorter survival times for patients with primary operable triple-negative breast cancer. Annals of Oncology 20, 1639–1646.

Machide, M., Kamitori, K., Kohsaka, S., 2000. Hepatocyte growth factor-induced differential activation of phospholipase cgamma 1 and phosphatidylinositol 3-kinase is regulated by tyrosine phosphatase SHP-1 in astrocytes. The Journal of Biological Chemistry 275, 31392–31398.

Manders, P., Beex, L.V., Tjan-Heijnen, V.C., Geurts-Moespot, J., Van Tienoven, T.H., Foekens, J.A., Sweep, C.G., 2002. The prognostic value of vascular endothelial growth factor in 574 node-

negative breast cancer patients who did not receive adjuvant systemic therapy. British Journal of Cancer 87, 772–778.
Markova, B., Albers, C., Breitenbuecher, F., Melo, J.V., Brummendorf, T.H., Heidel, F., Lipka, D., Duyster, J., Huber, C., Fischer, T., 2010. Novel pathway in Bcr-Abl signal transduction involves Akt-independent, PLC-gamma1-driven activation of mTOR/p70S6-kinase pathway. Oncogene 29, 739–751.
Marrero, M.B., Venema, R.C., Ma, H., Ling, B.N., Eaton, D.C., 1998. Erythropoietin receptor-operated Ca2+ channels: activation by phospholipase C-gamma 1. Kidney International 53, 1259–1268.
Mason, I., 2000. The RET receptor tyrosine kinase: activation, signalling and significance in neural development and disease. In. Pharm Acta Helv Vol. 74, 261–264.
Miles, D.W., Chan, A., Dirix, L.Y., Cortes, J., Pivot, X., Tomczak, P., Delozier, T., Sohn, J.H., Provencher, L., Puglisi, F., Harbeck, N., Steger, G.G., Schneeweiss, A., Wardley, A.M., Chlistalla, A., Romieu, G., 2010. Phase III study of bevacizumab plus docetaxel compared with placebo plus docetaxel for the first-line treatment of human epidermal growth factor receptor 2-negative metastatic breast cancer. Journal of Clinical Oncology 28, 3239–3247.
Miller, K., Wang, M., Gralow, J., Dickler, M., Cobleigh, M., Perez, E.A., Shenkier, T., Cella, D., Davidson, N.E., 2007. Paclitaxel plus bevacizumab versus paclitaxel alone for metastatic breast cancer. The New England Journal of Medicine 357, 2666–2676.
Nel, A.E., Gupta, S., Lee, L., Ledbetter, J.A., Kanner, S.B., 1995. Ligation of the T-cell antigen receptor (TCR) induces association of hSos1, ZAP-70, phospholipase C-gamma 1, and other phosphoproteins with Grb2 and the zeta-chain of the TCR. The Journal of Biological Chemistry 270, 18428–18436.
Pocock, T.M., Bates, D.O., 2001. In vivo mechanisms of vascular endothelial growth factor-mediated increased hydraulic conductivity of Rana capillaries. The Journal of Physiology 534, 479–488.
Poulin, B., Sekiya, F., Rhee, S.G., 2000. Differential roles of the Src homology 2 domains of phospholipase C-gamma1 (PLC-gamma1) in platelet-derived growth factor-induced activation of PLC-gamma1 in intact cells. The Journal of Biological Chemistry 275, 6411–6416.
Ren, H.Y., Komatsu, N., Shimizu, R., Okada, K., Miura, Y., 1994. Erythropoietin induces tyrosine phosphorylation and activation of phospholipase C-gamma 1 in a human erythropoietin-dependent cell line. The Journal of Biological Chemistry 269, 19633–19638.
Rouzier, R., Perou, C.M., Symmans, W.F., Ibrahim, N., Cristofanilli, M., Anderson, K., Hess, K.R., Stec, J., Ayers, M., Wagner, P., Morandi, P., Fan, C., Rabiul, I., Ross, J.S., Hortobagyi, G.N., Pusztai, L., 2005. Breast cancer molecular subtypes respond differently to preoperative chemotherapy. Clinical Cancer Research 11, 5678–5685.
Sala, G., Dituri, F., Raimondi, C., Previdi, S., Maffucci, T., Mazzoletti, M., Rossi, C., Iezzi, M., Lattanzio, R., Piantelli, M., Iacobelli, S., Broggini, M., Falasca, M., 2008. Phospholipase Cgamma1 is required for metastasis development and progression. Cancer Research 68, 10187–10196.
Tomlinson, M.G., Kane, L.P., Su, J., Kadlecek, T.A., Mollenauer, M.N., Weiss, A., 2004. Expression and function of Tec, Itk, and Btk in lymphocytes: evidence for a unique role for Tec. Molecular and Cellular Biology 24, 2455–2466.
Volk, L.D., Flister, M.J., Bivens, C.M., Stutzman, A., Desai, N., Trieu, V., Ran, S., 2008. Nab-paclitaxel efficacy in the orthotopic model of human breast cancer is significantly enhanced by concurrent anti-vascular endothelial growth factor A therapy. Neoplasia 10, 613–623. New York, NY.
von Minckwitz, G., Eidtmann, H., Rezai, M., Fasching, P.A., Tesch, H., Eggemann, H., Schrader, I., Kittel, K., Hanusch, C., Kreienberg, R., Solbach, C., Gerber, B., Jackisch, C., Kunz, G., Blohmer, J.-U., Huober, J., Hauschild, M., Fehm, T., Muller, B.M., Denkert, C., Loibl, S., Nekljudova, V., Untch, M., 2012. Neoadjuvant chemotherapy and bevacizumab for HER2-Negative breast cancer. New England Journal of Medicine 366, 299–309.
Weber, J.R., Bell, G.M., Han, M.Y., Pawson, T., Imboden, J.B., 1992. Association of the tyrosine kinase LCK with phospholipase C-gamma 1 after stimulation of the T cell antigen receptor. The Journal of Experimental Medicine 176, 373–379.
Williams, B.L., Irvin, B.J., Sutor, S.L., Chini, C.C., Yacyshyn, E., Bubeck Wardenburg, J., Dalton, M., Chan, A.C., Abraham, R.T., 1999. Phosphorylation of Tyr319 in ZAP-70 is required for T-cell antigen receptor-dependent phospholipase C-gamma1 and Ras activation. The EMBO Journal 18, 1832–1844.
Workman, P., Aboagye, E.O., Balkwill, F., Balmain, A., Bruder, G., Chaplin, D.J., Double, J.A., Everitt, J., Farningham, D.A., Glennie, M.J., Kelland, L.R., Robinson, V., Stratford, I.J., Tozer, G.M., Watson, S., Wedge, S.R., Eccles, S.A., 2010. Guidelines for the welfare and use of animals in cancer research. British Journal of Cancer 102, 1555–1577.
Xie, Z., Chen, Y., Liao, E.Y., Jiang, Y., Liu, F.Y., Pennypacker, S.D., 2010a. Phospholipase C-gamma1 is required for the epidermal growth factor receptor-induced squamous cell carcinoma cell mitogenesis. Biochemical and Biophysical Research Communications 397, 296–300.
Xie, Z., Peng, J., Pennypacker, S.D., Chen, Y., 2010b. Critical role for the catalytic activity of phospholipase C-gamma1 in epidermal growth factor-induced cell migration. Biochemical and Biophysical Research Communications 399, 425–428.
Yanagisawa, M., Yorozu, K., Kurasawa, M., Nakano, K., Furugaki, K., Yamashita, Y., Mori, K., Fujimoto-Ouchi, K., 2010. Bevacizumab improves the delivery and efficacy of paclitaxel. Anti-cancer Drugs 21, 687–694.
Yang, J.M., Vassil, A.D., Hait, W.N., 2001. Activation of phospholipase C induces the expression of the multidrug resistance (MDR1) gene through the Raf-MAPK pathway. Molecular Pharmacology 60, 674–680.
Yang, S.X., Steinberg, S.M., Nguyen, D., Wu, T.D., Modrusan, Z., Swain, S.M., 2008. Gene expression profile and angiogenic marker correlates with response to neoadjuvant bevacizumab followed by bevacizumab plus chemotherapy in breast cancer. Clinical Cancer Research 14, 5893–5899.